Measurement and Calibration of Droplet Size Distributions in Water−in−Oil Emulsions by Particle Video Microscope and a Focused Beam Reflectance Method

ARTICLE *in* INDUSTRIAL & ENGINEERING CHEMISTRY RESEARCH · DECEMBER 2009

Impact Factor: 2.59 · DOI: 10.1021/ie901228e

5 AUTHORS, INCLUDING:

Carolyn Ann Koh
Colorado School of Mines
199 PUBLICATIONS **5,181** CITATIONS
SEE PROFILE

David Wu
Colorado School of Mines
99 PUBLICATIONS **1,672** CITATIONS
SEE PROFILE

Measurement and Calibration of Droplet Size Distributions in Water-in-Oil Emulsions by Particle Video Microscope and a Focused Beam Reflectance Method

John A. Boxall,[†] Carolyn A. Koh,[†] E. Dendy Sloan,[†] Amadeu K. Sum,*[,†] and David T. Wu*[,†,‡]

Center for Hydrate Research, Department of Chemical Engineering, and Department of Chemistry, Colorado School of Mines, Golden, Colorado 80401

Water droplet sizes in crude oil emulsions were measured using an in situ particle video microscope (PVM) probe and a focused beam reflectance measurement (FBRM) probe for a variety of oils spanning over two orders of magnitude in viscosity and for varying shear rates. The arithmetic or Sauter mean diameter was found to maintain the same constants of proportionality with the maximum (99th percentile) droplet size for different distributions, previously only shown for water-continuous emulsions. The FBRM values for the mean droplet size, while lower than the PVM values, could be related to the latter by an empirical quadratic relationship with an average error of less than 20%. The droplet size distribution was found to be represented well by a log-normal distribution with good agreement between correlated and measured mean droplet size. Following the agreement between the mean and maximum droplet sizes, the log-normal standard deviation was linearly related to the mean droplet size. The PVM probe was found to be a useful tool for determining droplet sizes in water-in-oil emulsions and as a calibration method for the FBRM probe. The droplet sizes measured provide a useful set of data for comparison with predictive models to determine the mean size or full droplet size distributions.

Introduction

The formation of emulsions impacts many facets of oil production, and droplet size has important implications for many of the problems that emulsions may cause. Production issues caused by emulsions come at a cost in terms of chemicals required or production lost.[1] The size of the water droplets dispersed in the emulsion is an important quantity, as it can affect both the stability and the rheology of the emulsion. The water droplet size in water-in-oil emulsions is also an important quantity for determining the surface area for gas hydrate formation in oil-dominated systems, as mass and heat transfer processes across this interface dominate formation rates.[2] In addition, an ability to determine the droplet size can be an important step in engineering the droplet size for creating small transportable hydrate particles, as required for cold flow applications suggested by ExxonMobil[3,4] and BP/Sintef/StatoilHydro.[5,6] In this work the size of water droplets was determined in a continuous crude oil phase for water volume fractions in a range from 10% to 20% and eight different oils using both a particle video microscope (PVM) probe and a focused beam reflectance measurement (FBRM) probe.

Zhou and Kresta[7] presented a review of measurements and correlations for droplet size in liquid−liquid mixing tanks using many different measurement techniques including light transmittance,[8] photographs,[9] and a Coulter counter.[10] In the examples given by Zhou and Kresta,[7] the dispersed phase (or droplets) was the higher viscosity (oil) phase and the continuous phase was typically water. With a low viscosity continuous phase, the inertial effects dominate droplet break-up, as viscous effects are very small.[11] The reverse emulsion (i.e., water-in-oil) consists of the higher viscosity oil as the continuous phase, which can result in the viscous forces becoming dominant. Although methods are available for determining droplet sizes in oil-continuous emulsions, such as video-enhanced microscopy[12] or NMR,[13] most require sampling of the emulsion before measurement. The FBRM and PVM particle size analysis probes provide an in situ measurement of the droplet sizes.[14]

Sprow[10] suggested that proportionality exists between the mean and the maximum size of the droplet size distribution, an observation based on their system of iso-octane and salt water. This observation was also reported by Brown and Pitt,[15] Calabrese et al.,[16] and Lemenand et al.,[17] among others, for emulsions with a continuous aqueous phase. Proportionality between the mean and maximum droplet sizes is shown in this work for oil-continuous emulsions. This proportionality allows a theory for the maximum droplet size to be applied to the mean droplet size with an addition of a prefactor. The arithmetic mean $\bar{d}$, or the Sauter mean, d_{32}, droplet diameters are more useful properties of the water-in-oil emulsion for characterizing the droplet size distribution, $p(d)$, and the surface area of droplets:

$$\bar{d} = \sum d \times p(d) \tag{1}$$

$$d_{32} = \sum d^3 \times p(d) / \sum d^2 \times p(d) \tag{2}$$

A comparison of the FBRM measured size distribution with both microscopic images and PVM images for both a known size distribution of glass beads and emulsion droplets was performed by Greaves et al.[14] The FBRM distribution measured for the glass particles showed an oversizing of the particles. However, the FBRM distribution measured for the water-in-oil emulsion showed that the droplet size distribution, measured using the PVM, is vastly undersized by the FBRM technique. The continuous oil phase was the same for both PVM and FBRM measurements, and the size range of the droplets/glass particles were very similar, so the different FBRM measurements must stem from how the laser is reflected by the FBRM probe for the different dispersed phases. This work serves as an example of the need to calibrate the FBRM. The relationship

* To whom correspondence should be addressed. (A.K.S.) Tel: +1 (303) 273-3873. Fax: +1 (303) 273-3730. E-mail: asum@mines.edu. (D.T.W.) Tel: +1 (303) 384-2066. Fax: +1 (303) 273-3730. E-mail: dwu@mines.edu.

† Center for Hydrate Research, Department of Chemical Engineering.

‡ Department of Chemistry.

10.1021/ie901228e
Published on Web 12/18/2009

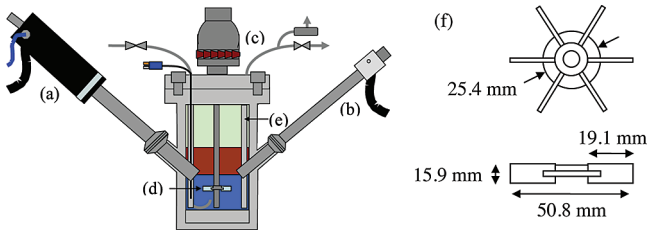

Figure 1. Schematic of mixing cell setup with (a) PVM probe, (b) FBRM probe, (c) magnedrive agitator, (d) 6-blade turbine impeller, (e) baffles (four), and (f) impeller dimensions.

between the FBRM measured droplet sizes and actual droplet sizes is very important, as the FBRM probe is often used in industrial applications where a PVM does not have the necessary safety classification.

Experimental Method

Droplet measurements were performed in a mixing cell (0.102 m internal diameter, 0.229 m height) with a single six-blade impeller (0.051 m diameter) 50.8 mm from the bottom of the cell. The baffles (four) were 1/10th the internal diameter of the cell and the same height as the cell. The cell has two particle size analysis probes oriented at opposite sides of the cell, a particle video microscope (PVM) probe, and a focused beam reflectance measurement (FBRM) probe placed at 45° angles into the cell at a level equal to the top of the impeller to maximize flow past the window and facilitate representative measurements of the system. Figure 1 shows a schematic diagram of the mixing cell with the probes. Figure 1f provides the dimensions for the six-bladed turbine impeller used in the mixing cell.

The experiments were performed by adding 680 mL of the crude oil and 120 mL of deionized water to the autoclave cell (15 vol% water). The cell was sealed and placed in the water bath kept at 20 °C and atmospheric pressure. The single six-blade turbine was set to a mixing speed of 300 rpm and kept at this speed until a steady droplet size was achieved, as determined by insignificant changes in the FBRM distribution. Typically this was reached within 3 h after mixing began or after the impeller speed was increased. The transient behavior of the droplet size distribution was not considered in this study. PVM images were recorded before increasing the impeller speed to 400 rpm. This process was repeated for 300, 400, 500, and 600 rpm impeller speeds. The stirred cell Reynolds numbers ranged from 50 to 15 400, with an average value of 3100. Weber numbers ranged from 130 to 730, with an average of 340.

Experiments measuring the droplet size were also performed using two impellers with the same geometry, spaced at 50.8 and 127.0 mm from the bottom of the cell. The fluid load in the cell was 770 and 410 mL of oil and water, respectively. The use of two impellers requires the Weber number to be doubled, assuming the impellers acted independently, which was shown via CFD simulations in another study.[18]

Focused Beam Reflectance Measurement (FBRM) Probe. The FBRM probe used in this study is a Mettler-Toledo Lasentec D600X particle size analyzer. A Class I, 3 MW laser with wavelength 791.8 nm is transmitted through fiber-optics to the probe tip. A rotating optical lens at the probe tip deflects the laser as shown in Figure 2a. When the probe is inserted into a system of droplets or particles, the laser emitted is reflected if it scans across the surface of a particle, as shown in Figure 2b. The probe measures the reflectance time and determines the chord length by the product of the time and the laser scan speed (scan speed set to 2 m/s). Further information on the FBRM can be found elsewhere.[19]

For all FBRM measurements, the focal point of the laser was set to −20 μm from the probe window using the calibration technique as suggested in the FBRM User's Manual.[19] The choice of −20 μm corresponds to the standard focal length as suggested by the manufacturer. This calibration was rechecked directly prior to experiments.

Particle Video Microscope (PVM) Probe. A complementary particle size analysis probe, the particle video microscope (PVM), also from Mettler-Toledo Lasentec, was used in this work. The PVM consists of six near-IR lasers which illuminate a small area in front of the probe face (Figure 3a). The probe records digital images of the illuminated area with a field of view of 826 μm × 619 μm. Droplets and particles larger than 20 μm can be clearly identified and measured from the PVM images; below this size scale, it can be difficult to distinguish individual drops (Figure 3b). Further information can be found in the PVM User's manual.[20]

Determining Droplet Size from the PVM Measurements. The actual droplet size distributions of the water-in-oil emulsions were determined using images from the PVM probe. Approximately 40 images were randomly taken for each distribution once a steady distribution was reached, and 150−400 droplets were counted to obtain the droplet size distributions (number counted depended on the number of droplets per image). Image J, an image analysis application, was used to determine the droplet size distribution from the images. Figure 4 shows two sample images with the droplets identified marked with a white center line. The image analysis provided a droplet

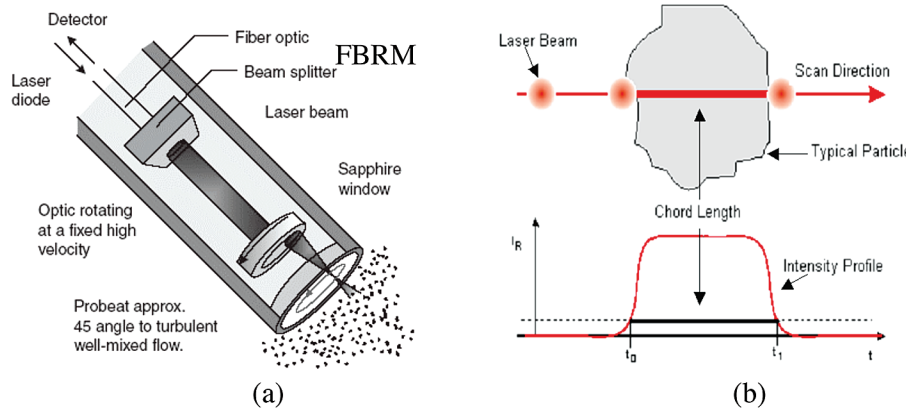

Figure 2. (a) Details of the FBRM probe technique. (b) Measurement of a particle chord length using the FBRM technique (provided by Mettler-Toledo Autochem, Inc.).

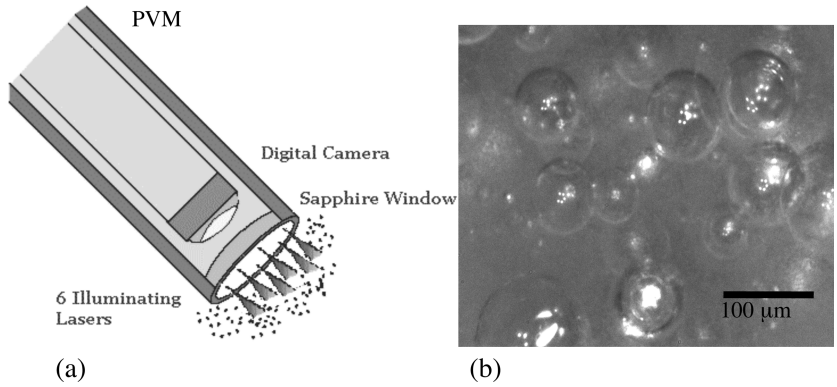

Figure 3. (a) Details of the PVM probe with six illuminating lasers. (b) Sample image given by the PVM probe.

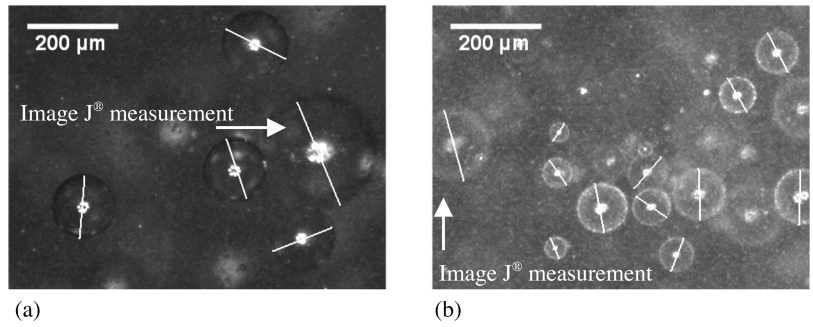

Figure 4. Sample PVM images of water-in-oil emulsions processed with Image J. Center lines are marked by Image J as identification of droplets. (a) Conroe oil and (b) Troika oil with 15% water cut at 400 rpm.

Table 1. Properties of the Crude Oils at 20 °C and 1 atm Used in the Droplet Size Measurements

fluid	density (kg/m^3)	interfacial tension[a] (mN/m)	viscosity (cP)
pure Conroe	842	20	3.1
20% Conroe with 80% CyC6	788	20	1.3
20% Conroe with 80% CP 70	854	20	15
20% Conroe with 80% CP 200	857	20	24
20% Conroe with 80% CP 500	864	20	83
20% Conroe with 80% Brightstock	886	20	262
Troika	869	11	20
Petronius	883	13	100

[a] Measured in deionized water.

size distribution in terms of pixels, and the calibration to transform pixels to actual size (μm) is given by the full width of an image measured (1280 pixels), which corresponds to an actual size of 826 μm (provided by Mettler-Toledo Lasentec). This scale corresponds to a calibration of 0.645 μm/pixel.

Crude Oil Properties. Table 1 summarizes the properties for the oils used in the experiments, including the blended oils. The objective of using the blends of crude oil with mineral oil was to retain the interfacial properties of the crude oil while changing the bulk viscosity of the mixture. Six different blends of the Conroe oil with different viscosity mineral oils were used; viscosities ranged from 1.3 cP with cyclohexane (CyC6) to 262 cP with Brightstock lubricant base oil. The medium viscosity mineral oils (CP 70, CP 200, and CP 500) refer to Crystal Plus white mineral oils obtained from STE Oil Company, Inc. The mineral oil samples obtained were all technical grade. Densities were measured using an oscillating U-tube densitometer (Anton-Parr DMA 4500 M). Although densities (788 kg/m^3 with CyC6 to 886 kg/m^3 with the Brightstock) varied slightly, these variations were negligible for these tests. The interfacial tensions were the same for all six of the Conroe blends (20 mN/m) and were measured by a CAM 200 optical contact angle meter (KSV Instrument). Interfacial tensions were measured from images of a crude oil droplet expelled from a syringe tip in a water phase. A pendant drop shape analysis was performed where the shape factor was defined through the Young−Laplace equation.[21] Viscosities were measured using a TA Instruments AR-G2 rheometer with a cone and plate geometry.

Results and Discussion

All experimental results shown below were performed using the mixing cell shown in Figure 1 with a single six-blade turbine impeller, except for some experiments in which two impellers (with same dimensions as given in Figure 1) were used.

Repeatability and Reproducibility of Measurements. The process of determining the droplet size from the PVM images required the manual measurement of droplet diameters using Image J. Figure 5 shows the comparisons of the PVM droplet size distributions between two independent analyses (i.e., analyzers 1 and 2). Three of the experiments were repeated to determine (1) the reproducibility of the method and (2) the repeatability of determining the PVM size distribution from a given set of PVM images. The three oils chosen for data reproduction were the Conroe (pure), Conroe with CP70, and Conroe with CP200. Figure 5 shows the good repeatability and the reproducibility of the droplet size measurements for the Conroe oils. The repeatability and reproducibility of the measurements were found to be reasonable with an average difference of 8.4% between the experiment repeats and an average difference of 5.1% between the analyzers.

Effect of Dispersed Phase Volume Fraction. The effect that the dispersed phase concentration has on the resulting droplet size has gained much attention in theoretical and experimental work on dispersions. The noncoalescing system of Brown and Pitt[15] showed no significant effect from the dispersed phase volume fraction from 0.05 to 0.2. Vankova et al.[22] showed that

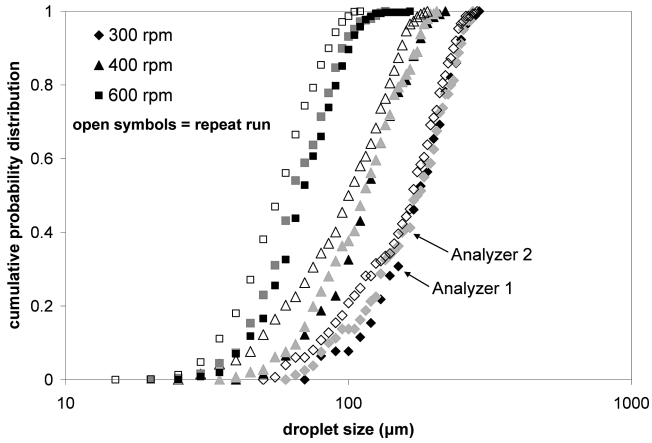

Figure 5. Conroe oil with 15% water cut showing the repeatability and reproducibility of two independent analyses of the PVM images. Open symbols indicate separate experiments and light/dark filled symbols indicate independent analysis.

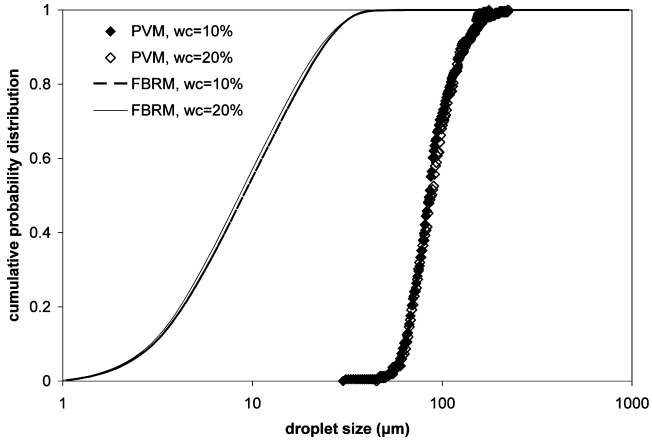

Figure 6. FBRM and PVM comparison of the water-in-oil emulsion with the Conroe oil as the continuous phase at different water cuts.

when stabilized oil droplet emulsions in a water phase were used, the dispersed phase volume fraction did not have a significant effect on the measured droplet size until approximately 50 vol%.

Here, the water volume fraction is referred to as the water cut and is defined as the water fraction in the total liquid volume. A water cut of 15% was used for all of the droplet size distribution measurements in this work. To confirm that the results were independent of the water cut, experiments with the pure Conroe oil were performed with 10% and 20% water cuts (deionized water) at 20 °C and 400 rpm. Figure 6 shows that both the PVM and the FBRM distributions for the two water cuts were indistinguishable. As such, a water cut of 15% was used for all other measurements as it was determined to give suitable PVM images without being too sparse at high droplet sizes or too dense with small droplets.

Mean Size Comparison between FBRM and PVM. Greaves et al.[14] showed that droplets in a water-in-oil emulsion were dramatically undersized by the FBRM probe. A comparison between the PVM measured droplet size and the FBRM distribution was performed with the droplet measurements. Figure 7 compares the mean of the FBRM measured distribution and the mean of the actual (PVM measured) droplet size for the different oils and impeller mixing speeds. As the data given in Figure 7 shows, the FBRM probe undersizes droplet diameters (for the >12 μm sizes measured). The PVM probe is limited to droplets larger than approximately 20 μm so there could be a contribution from smaller satellite droplets that are unaccounted for with the PVM distribution but measured by the FBRM probe (which has a lower limit of 0.5 μm). Although these smaller droplets cannot be accounted for in the PVM measured distribution, their presence would still be detectable, as interference. The mean droplet size would be slightly overestimated with the PVM by not including these smallest droplets, but this would not fully account for the undersizing of the droplets that was found by the FBRM probe. The maximum size measured by the FBRM was still considerably smaller than the droplets present, as seen by the PVM.

A second-order polynomial (eq 3) was fit to the Conroe oil data with an average absolute percentage error between the PVM measured and correlated mean diameters of 17.2%. A power law function (eq 4) was also fit to the Conroe oil data with an average absolute percentage error between the PVM measured and correlated mean diameters of 17.9%.

$$\text{PVM mean} = 0.1481 \times (\text{FBRM mean})^2 + 2.9804 \times (\text{FBRM mean}) \quad (3)$$

$$\text{PVM mean} = 1.1455 \times (\text{FBRM mean})^{1.5469} \quad (4)$$

Figure 8 provides an analysis of the error between the measured and calibrated mean droplet sizes (using either eq 3 or 4). The error [(measured − calibrated)/measured], is plotted against both the measured droplet mean size (Figure 8a) and the mixing speed (Figure 8b). The error analysis shows that

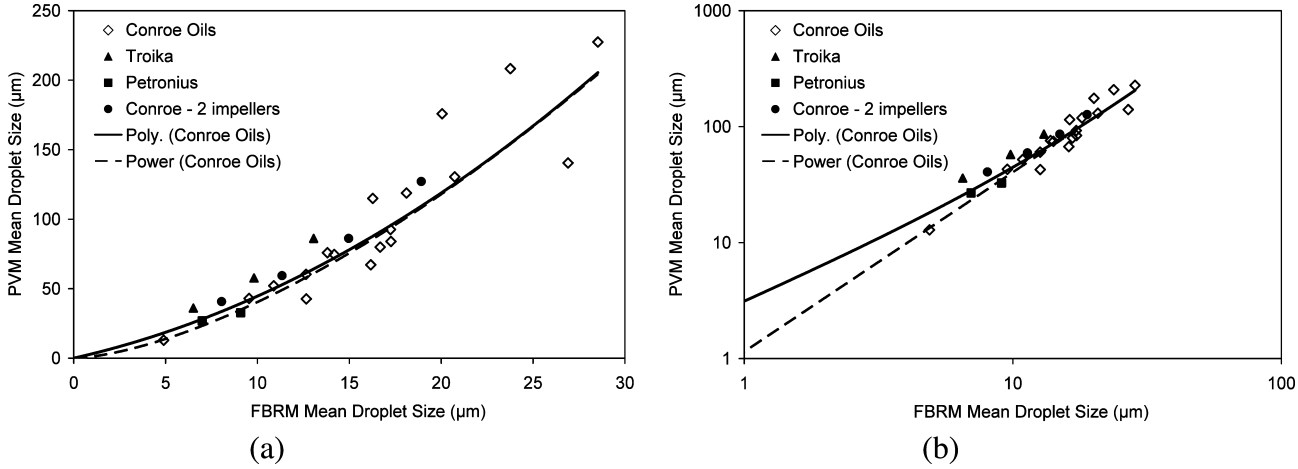

Figure 7. Calibration of FBRM to PVM particle size for the different oils: (a) rectilinear axes, (b) log−log axes.

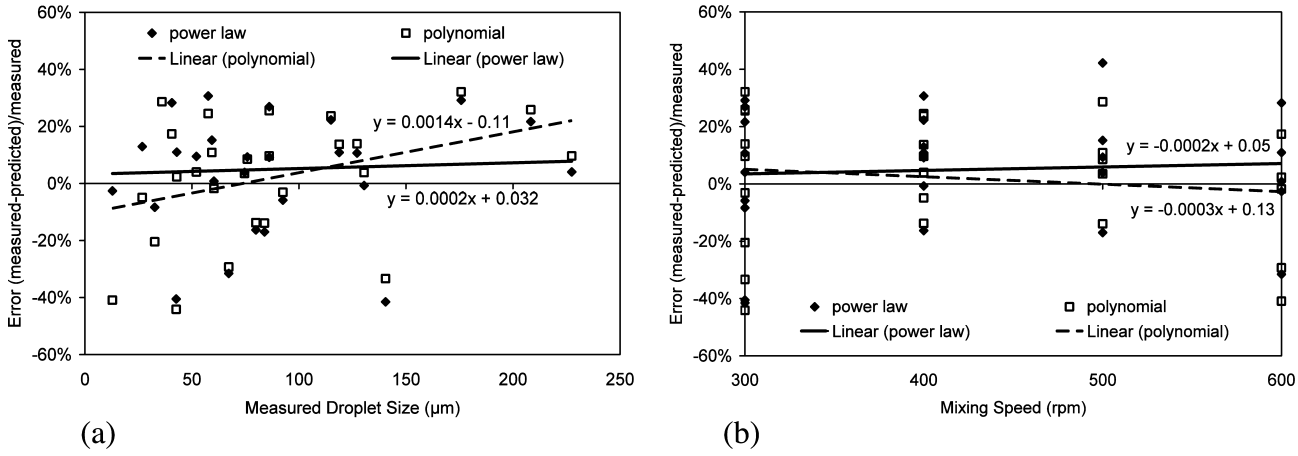

Figure 8. Error in the polynomial and power-law correlations as a function of (a) droplet size and (b) mixing speed.

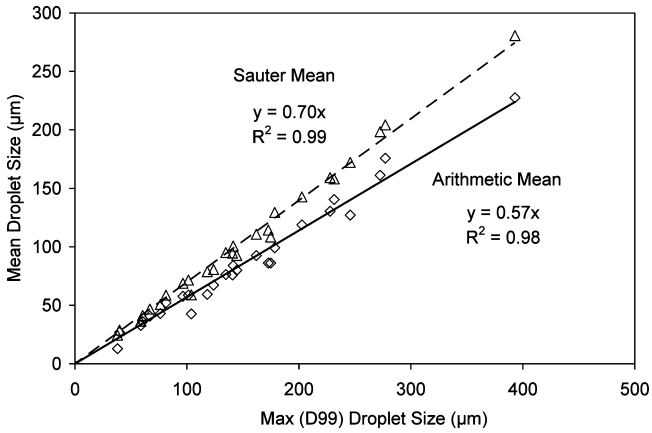

Figure 9. Linear correlation between the mean diameter (diamonds: arithmetic, triangles: Sauter) and the maximum (D99) droplet sizes measured by the PVM probe.

there is a slight dependence of the polynomial fit on the droplet size, but negligible dependence for the power law, although both underpredict the size of droplets larger than 150 μm. Neither empirical calibration shows any dependence on the mixing speed.

Note that the calibration is specific to droplets of water in oil, but it was shown to be applicable for two different types of mixing (single impeller, and two impellers) and a variety of crude oils (Figure 7). Greaves et al.[14] showed that the response of the FBRM is significantly different for water droplets in oil compared to hollow glass beads; whereas the droplets were significantly undersized (as shown in Figure 7), the glass beads were oversized by the FBRM with chords measured that were greater than the diameters of the actual particles present.

Relationship between Mean and Maximum Droplet Size. The mean droplet size and the maximum droplet sizes are well correlated between each other. Figure 9 shows that a linear relationship correlates the PVM mean droplet size and the 99th percentile (D99) droplet size. This suggests that the mean and maximum sizes (D99, as defined here) differ by a constant (0.57), and that the mean and maximum sizes of the distribution can be interchanged for comparison with droplet correlations, which often describe the maximum stable droplet size. An equivalent comparison between the maximum (D99) and the Sauter mean diameter is also shown in Figure 9, with a proportionality constant of 0.70.

The constant of proportionality between the Sauter mean diameter and maximum size agrees well with values reported in the literature. Sprow,[10] Brown and Pitt,[15] Calabrese et al.,[16] and Lemenand et al.[17] reported proportionality constant values of 0.38, 0.7, 0.48−0.6, and 0.48, respectively. Giapos et al.[23] and Zhou and Kresta[7] also reported a collection of values within this range. The constant of 0.70 found in this work represents the higher end of this range of constants, which corresponds to a tighter distribution with less breadth. As discussed above, the water-in-oil emulsions here are believed to be noncoalescing, much like the system of Brown and Pitt,[15] who reported that their system does not coalesce. The smaller breadth observed

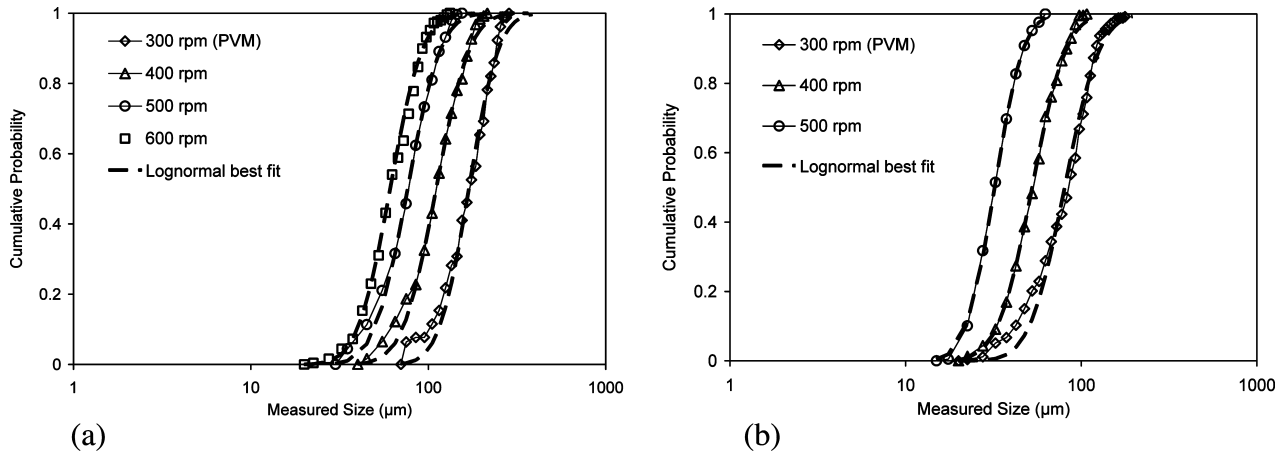

Figure 10. Comparison of PVM droplet distribution droplet size and best fit with log-normal distributions for (a) pure Conroe and (b) Troika oils.

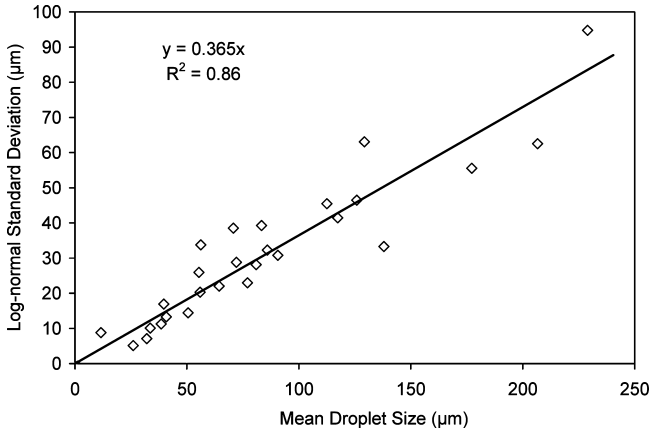

Figure 11. Linear correlation of arithmetic mean size versus standard deviation for log-normal distribution.

in the results here could be attributed to the noncoalescing nature of the system.

Full Droplet Size Distribution. The full droplet size distribution was determined to be well described by a log-normal distribution, as shown in Figure 10. The arithmetic mean diameter of the PVM measured droplet size distributions agreed very well with the mean droplet diameter for the best fit log-normal distribution with an average absolute percentage error between the two means of 3.6%. Following the proportionality between the maximum and mean droplet diameters, the standard deviation for the log-normal distribution was approximately proportional to the mean droplet size (Figure 11).

Measured Droplet Size as a Function of RPM and Viscosity. The results for the droplet size measurements are summarized in Table 2. The measured droplet sizes are given as a function of the different crude oils, with properties given in Table 1, and for different impeller speeds.

The droplet size data are unique, as only a limited amount of published data exists for droplet size measurements as a function of increasing continuous phase viscosity. Stamatoudis and Tavlarides,[24] and later Vankova et al.,[22] presented droplet size measurements for oil-in-water emulsions with the continuous aqueous phase adjusted using glycerol. Here, the continuous phase viscosity is increased over 2 orders of magnitude from 1.3 to 262 cP with a near constant continuous phase density and a constant interfacial tension between the continuous and dispersed phases (oil and water, respectively).

The droplet size results given in Table 2, along with the properties given in Table 1, provide a comprehensive set of data for comparison with droplet size prediction models suggested by Hinze[11] for the inertial subrange, and by Shinnar[25] for the viscous subrange. This comparison is the subject of another contribution.[26]

Conclusions

This study considered measurements of the droplet size distribution for water-in-oil emulsions using the PVM probe for different crude oils with a wide variety of viscosities. The PVM probe was found to be a useful tool for determining the droplet size distribution in dark crude oils.

A correlation between the measurement of the droplet size using the PVM and FBRM particle size analysis probes for droplet measurements was determined here. In previous studies, the droplet size was shown to be dramatically undersized by the FBRM probe, even taking into account that it measures chord lengths rather than actual sizes. An empirical fit was found to give reasonable agreement between the FBRM and PVM mean sizes measured for droplets with an average error less than 20%.

The measured droplet size distribution was determined to be independent of the dispersed phase volume fraction for the range 10−20 vol%. The mean and maximum droplet sizes were found to be proportional to one another for both arithmetic and Sauter mean diameters. The droplet size distribution is typically a well-behaved distribution with the log-normal distribution shown to consistently represent the complete droplet size distribution.

Table 2. Measured Droplet Size for the Different Crude Oils Using the FBRM and PVM Particle Size Analysis Probes

		FBRM	PVM		
fluid	impeller speed (rpm)	mean (μm)	Arithmetic mean (μm)	Sauter mean (μm)	D99 (μm)
pure Conroe	300	20.0	175.8	204.3	277.2
	400	18.1	118.8	142.6	202.7
	500	17.3	83.9	100.6	141.3
	600	16.2	67.2	80.6	123.8
20% Conroe with 80% CyC6	300	23.8	208.3	248.0	313.6
	400	16.3	115.0	143.6	208.7
	500	14.2	74.6	107.5	197.1
	600	12.6	60.3	91.1	143.8
20% Conroe with 80% CP 70	300	28.5	227.4	280.6	393.1
	400	20.7	130.4	159.2	227.9
	500	13.8	75.9	94.7	140.7
	600	9.5	42.9	50.7	76.3
20% Conroe with 80% CP 200	300	26.9	140.5	158.0	231.5
	400	16.7	79.9	92.5	144.5
20% Conroe with 80% CP 500	300	17.2	92.5	110.6	161.9
	400	10.9	52.1	58.6	81.2
20% Conroe with 80% Brightstock	300	12.7	42.6	58.9	103.9
	600	4.9	12.9[a]	24.4[a]	38.0[a]
Troika	300	13.1	86.1	108.3	174.9
	400	9.8	57.6	68.9	96.4
	500	6.5	36.0	41.3	60.4
Petronius	300	9.1	32.6	36.3	58.8
	400	7.0	26.8	28.7	39.8
pure Conroe: two impellers	300	18.9	127.1	172.2	245.9
	400	15.0	86.1	114.4	172.7
	500	11.3	59.3	78.7	118.2
	600	8.0	40.6	46.8	66.9

[a] Determined via microscope instead of PVM (too small for PVM).

Following the proportionality between the mean and maximum droplet sizes measured, the standard deviation for the log-normal distribution was also found to be proportional to the mean droplet size.

Acknowledgment

We thank Jon Monserud for his help in collecting and analyzing the PVM and FBRM images. The authors acknowledge Chevron ETC for the particle video microscope (PVM) probe. Also, we thank the Center for Hydrate Research consortium at the Colorado School of Mines (BP, Champion, Chevron, ConocoPhilips, ExxonMobil, Haliburton, Multichem, Nalco, Petrobras, Schlumberger, Shell, StatoilHydro, and Total) for funding this work. A.K.S. acknowledges the support of DuPont for a DuPont Young Professor Award.

Literature Cited

(1) Kokal, S. Crude-Oil Emulsions: A State-of-the-Art Review. *SPE Prod. Facil.* **2005**, *20*, 5.

(2) Sloan, E. D.; and Koh, C. A. *Clathrate Hydrates of Natural Gases*, 3rd ed.; CRC Press: Boca Raton, FL, 2008.

(3) Talley, L.; Turner, D.; Priedeman, D. J. Method of Generating a Non-Plugging Hydrate Slurry. US Patent 60/782,449, 2008.

(4) Turner, D.; Talley, L. Hydrate Inhibition Via Cold Flow - No Chemicals Or Insulation. Proceedings of the 6th International Conference on Gas Hydrates, Vancouver, British Columbia, Canada, July 6−10, 2008.

(5) Lund, A.; Lysne, D.; Larsen, R.; Hjarbo, K. W. Method and System for Transporting a Flow of Fluid Hydrocarbons Containing Water. Norwegian patent NO 311.854, British patent GB 2,358,640, Eurasian Patent 200100475, 2004.

(6) Wolden, M.; Lund, A.; Oza, N.; Makogon, T.; Argo, C. B.; Larsen, R. Cold Flow Black Oil Slurry Transport of Suspended Hydrate and Wax Solids. Proceedings of the 5th International Conference on Gas Hydrates, Trondheim, Norway, June 12−16, 2005.

(7) Zhou, G.; Kresta, S. M. Correlation of Mean Drop Size and Minimum Drop Size with the Turbulence Energy Dissipation and the Flow in an Agitated Tank. *Chem. Eng. Sci.* **1998**, *53*, 2063.

(8) Vermeulen, T.; Williams, G. M.; Langlois, G. E. Interfacial Area in Liquid-liquid and Gas-liquid Agitation. *Chem. Eng. Prog.* **1955**, *51*, 85.

(9) Chen, H. S.; Middleman, S. Drop Size Distribution in Agitated Liquid-Liquid Systems. *AIChE J.* **1967**, *13*, 989.

(10) Sprow, F. B. Distribution of Drop Sizes Produced in Turbulent Liquid-Liquid Dispersion. *Chem. Eng. Sci.* **1967**, *22*, 435.

(11) Hinze, J. O. Fundamentals of the Hydrodynamic Mechanism of Splitting in Dispersion Processes. *AIChE J.* **1955**, *1*, 289.

(12) Sjoblom, J., Ed. *Encyclopedic Handbook of Emulsion Technology*; Marcel Dekker, Inc.: New York, 2001; p 349.

(13) Aichele, C. P.; Flaum, M.; Jiang, T.; Hirasaki, G. J.; Chapman, W. G. Water in Oil Emulsion Droplet Size Characterization using a Pulsed Field Gradient with Diffusion Editing (PFG-DE) NMR Technique. *J. Colloid Interface Sci.* **2007**, *315*, 607.

(14) Greaves, D.; Boxall, J.; Mulligan, J.; Montesi, A.; Creek, J.; Sloan, E. D.; Koh, C. A. Measuring the Particle Size of a Known Distribution using the Focused Beam Reflectance Measurement Technique. *Chem. Eng. Sci.* **2008**, *63*, 5410.

(15) Brown, D. E.; Pitt, K. Drop Size Distribution of Stirred Non-Coalescing Liquid-Liquid System. *Chem. Eng. Sci.* **1972**, *27*, 577–583.

(16) Calabrese, R. V.; Chang, T. P. K.; Dang, P. T. Drop Breakup in Turbulent Stirred-Tank Contactors, Part I: Effect of Dispersed-Phase Viscosity. *AIChE J.* **1986**, *32* (4), 657.

(17) Lemenand, T.; Della Valle, D.; Zellouf, Y.; Peerhossaini, H. Droplets Formation in Turbulent Mixing of Two Immiscible Fluids in a New Type of Static Mixer. *Int. J. Multiphase Flow* **2003**, *29*, 813.

(18) Greaves D. The Effects of Hydrate Formation and Dissociation on High Water Content Emulsions, Masters Thesis, Colorado School of Mines, Golden CO, 2007.

(19) Mettler-Toledo Lasentec® Product Group. *Lasentec® D600 Hardware Manual*; Mettler-Toledo AutoChem, Inc.: Redmond, WA, 2001.

(20) Mettler-Toledo Lasentec® Product Group. *Lasentec® PVM User Manual*; Mettler-Toledo AutoChem, Inc.: Redmond, WA, 2002.

(21) Laidler, K. J.; Meiser, J. H. *Physical Chemistry*, 3rd ed.; Houghton Mifflin Co.: Boston, MA, 1999.

(22) Vankova, N.; Tcholakova, S.; Denkov, N. D.; Ivanov, I. B.; Vulchev, V. D.; Danner, T. Emulsification in turbulent flow 1. Mean and Maximum Drop Diameters in Inertial and Viscous Regimes. *J. Colloid Interface Sci.* **2007**, *312*, 363.

(23) Giapos, A.; Pachatouridis, C.; Stamatoudis, M. Effect of the Number of Impeller Blades on the Drop Sizes in Agitated Dispersions. *Trans. IChemE, Part A, Chem. Eng. Res. Des.* **1986**, *83* (A12), 1425.

(24) Stamatoudis, M.; Tavlarides, L. L. The Effect of Continuous Phase Viscosity on the Unsteady State Behavior of Liquid-liquid Agitated Dispersions. *Chem. Eng. J.* **1987**, *35*, 137.

(25) Shinnar, R. On the Behaviour of Liquid Dispersions in Mixing Vessels. *J. Fluid Mech.* **1961**, *10*, 259.

(26) Boxall, J.; Koh, C. A.; Sloan, E. D.; Sum, A. K.; Wu, D. T. Scaling of Droplet Size in Water-in-Oil Emulsions under Turbulent Flow. *Science* **2009**, submitted.

Received for review August 4, 2009
Revised manuscript received December 1, 2009
Accepted December 2, 2009

IE901228E